Isomers in the ^{123}Cd and ^{125}Cd decays and level schemes in ^{123}In and ^{125}In

H. Huck, A. Jech, G. Martí, M. L. Pérez, J. J. Rossi, and H. M. Sofía
Departamento de Física, Comisión Nacional de Energia Atómica, 1429 Buenos Aires, Argentina
(Received 26 April 1988)

Samples of ^{123,125}Cd were obtained by on-line mass separator techniques applied to natural U fast-neutron fission products. Special emphasis was devoted to half-life measurements of the ^{123,125}Cd decays and to the level schemes of ^{123,125}In. Two half-lives of 2.12 ± 0.03 s and 1.81 ± 0.03 s have been measured for decays of ^{123}Cd. Also, for decays of ^{125}Cd two half-lives of 0.68 ± 0.04 s and 0.48 ± 0.03 s were observed and measured. Four independent level schemes produced by the above-mentioned decays are proposed based upon the present results and previously reported data. The ^{123}In and ^{125}In level schemes are discussed within the hole-vibration coupling formalism, assuming a single hole coupled to the quadrupole surface vibrations of the corresponding ^{124}Sn and ^{126}Sn isotopes. The interaction between the hole and the vibrating core is treated perturbatively within the nuclear field theory formalism.

I. INTRODUCTION

The odd-mass neutron-rich In nuclei have been extensively investigated, both from nuclear reactions[1–4] and from Cd decay studies,[5–11] and their level schemes have been well established. The structure of the excited states in ^{115,117,119,121}In nuclei is particularly interesting because among the presence of the single-hole and single-hole plus quadrupole phonon vibrations states (Sn core), several low-lying deformed states were identified. The first indication of strongly deformed states was made by Bäcklin *et al.*[5] in ^{115,117}In. In both nuclei, they have identified two levels having spins and parities $\frac{1}{2}^+$ and $\frac{3}{2}^+$ as the first members of a strongly decoupled $K=\frac{1}{2}^+[431]$ band within the framework of the Nilsson model. Later Pandharipande *et al.*[6] further suggested the existence of three other members of that band in ^{117}In. McDonald *et al.*[8] and Fogelberg *et al.*[11] have also reported similar deformed states in ^{119}In and ^{121}In, respectively.

Following the systematic behavior of the lowest energy member of the band ($\frac{3}{2}^+$ level),[12] one can see that it reaches a minimum energy value in ^{117}In and ^{119}In (approximately at 600 keV in both nuclei),[8] increases 333 keV in ^{121}In,[11] and it is expected a further increase in energy for heavier In isotopes when the neutron number N, approaches the closed shell $N=82$. This would suggest a decreasing deformation character for these In isotopes, in agreement with the fact that the deformation depends on the number of protons and neutrons out of closed shell coupled through a proton-neutron quadrupole interaction. Therefore, it is of interest to study odd-mass In nuclei heavier than ^{121}In in order to test these predictions.

Recently an experiment was performed in order to study the decays of ^{123,125,127}Cd.[13] Level schemes of ^{123}In and ^{125}In have been suggested and the expected decreasing deformation was experimentally confirmed. It is also suggested that the possible lowest-lying member of the intruder band may have an excitation energy above 1600 keV in both nuclei.

On the other hand, the systematic decay of the odd-mass Cd isotopes from $A=115$ to 121 shows the existence of two β^--decaying isomers, one being the low-spin isomer ($\frac{1}{2}^+,\frac{3}{2}^+$) and the other being the high-spin

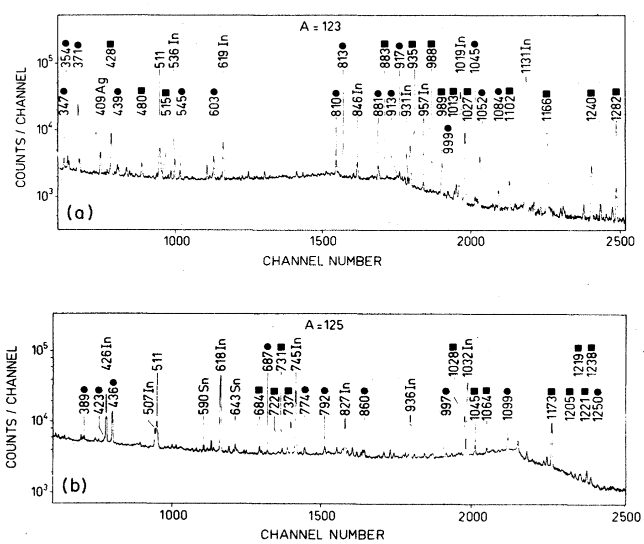

FIG. 1. (a) A relevant portion of the γ-ray spectrum recorded for the $A=123$ isobars. The recording was performing with the collecting tape moving continuously enhancing the ^{123}Cd decay activity with respect to the ^{123}In and ^{123}Sn decay activities. The solid circle and square correspond to transitions following the decay of ^{123}Cd^g (2.12 s) and ^{123}Cd^m (1.81 s), respectively. Transitions following the decays of ^{123}In and ^{123}Sn are also labeled. The γ-ray transition units are in keV. (b) The same as (a) but for the $A=125$ isobars. The solid circle and square correspond to transitions following the decay of ^{125}Cd^g (0.68 s) and ^{125}Cd^m (0.48 s), respectively. Transitions following the decays of ^{125}In and ^{125}Sn are also labeled. The γ-ray transition units are in keV.

 ©1989 The American Physical Society

isomer ($\frac{11}{2}^-$). The present results of the measured γ-ray transition intensities, following the decays of ^{123}Cd and ^{125}Cd, showed substantial discrepancies with the γ-ray intensities data of Refs. 13 and 14. A possible explanation is that the present mechanism to produce fission products based upon natural U fast-neutron fission favors high-spin isomer production and therefore two isomers were identified, whereas in Refs. 13 and 14 only one is assumed.

Simultaneously, with our experiments, Mach *et al.*[15] reported two half-lives measured in the ^{123}Cd decay and two half-lives measured in the ^{125}Cd decay. However, within their experimental errors, the half-life values of the ^{125}Cd decay were essentially the same.

Encouraged by those results, the experiments were following paying special attention to the half-lives mentioned above and to establish the level schemes for both ^{123,125}In isotopes. The assumption of decreasing deformation with increasing number of neutrons will be also discussed.

II. EXPERIMENTAL TECHNIQUES

The activities of masses 123 and 125 were obtained from fast-neutron fission of natural U using the NAVE (núcleos alejados del valle de estabilidad, i.e., nuclear far from the stability line) facility at the TANDAR laboratory. A more detailed description of the experimental performance can be found in Ref. 16. Only a brief description of the system will be given here.

Fast neutrons were produced from the Be(d,n) reaction, by bombarding a thick Be target with a deuteron beam of 30 MeV and 500 nA supplied by a 20 MV tandem accelerator.[17] The fast-neutrons flux impinged the ion source with the U sample incorporated,[18] where the fission products were produced, thermalized, ionized, and extracted. Afterward, they were analyzed by an electromagnetic mass separator, and finally collected on a moving aluminum coated mylar tape. The γ-ray detectors were placed close to the collecting point to allow direct on-line measurements.

Two HPGe γ-ray detectors were employed in our measurements. A 40% efficiency and 1.95 keV energy resolution (at 1.33 MeV) detector was used for recording single γ rays and multiscaling spectra associated with the half-life measurements. For coincidences, a 30% efficiency and 2.00 keV energy resolution (at 1.33 keV) gamma-X detector was also utilized. This last detector has been useful to identify characteristic x rays due to its low-energy extended range. Both detectors were placed in a 90° geometry.

The collector assembly was operated with different time schedules in order to vary the activity ratios according to the half-lives and parental relations. In this way it was possible to obtain a positive assignment for the γ radiation detected from the different decays present in both masses of interest.

The half-live measurements were performed from 16 consecutive spectra collected in a multiscaling mode, after each collection time. For mass 123 the collection time was 5 s. Immediately after, the beam was electrostatically deflected and simultaneously each decay spectrum was recorded during time intervals of 0.3–0.5 s. For mass 125 the time collection period was 3 s and each decay spectrum was recorded during 0.1–0.3 s. For both

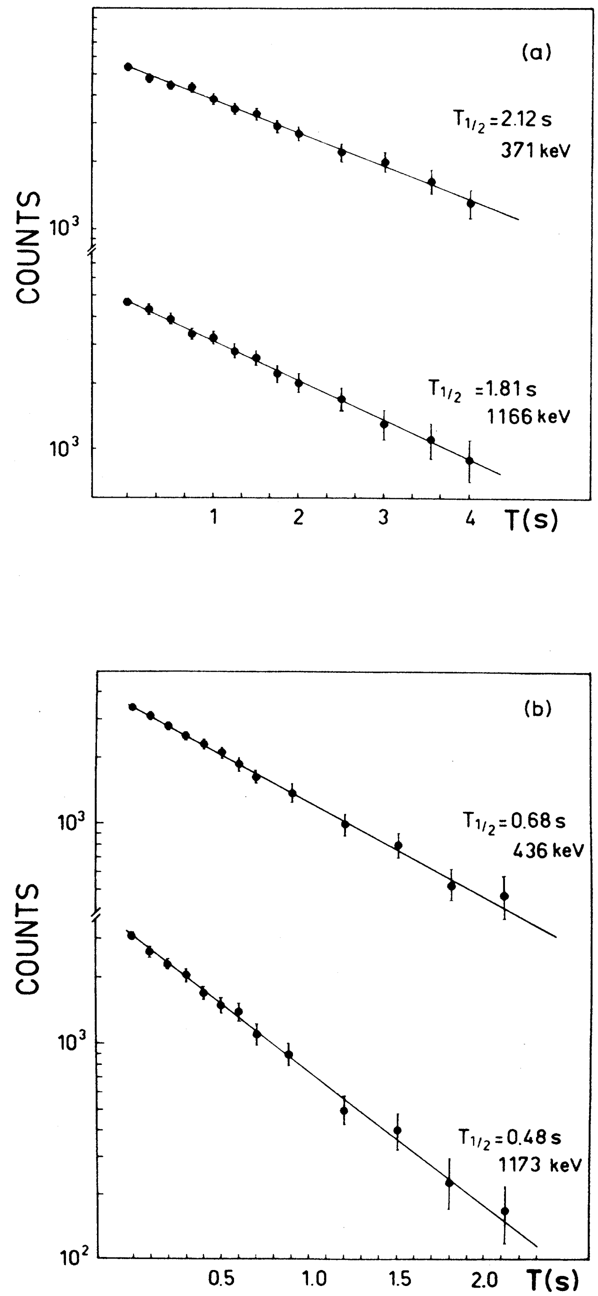

FIG. 2. (a) Decay curves of the most important γ transitions following the decay of ^{123}Cd^g (2.12 s) and ^{123}Cd^m (1.81 s). (b) The same as for the decay of ^{125}Cd^g (0.68 s) and ^{125}Cd^m (0.48 s).

TABLE I. γ-ray energies and intensities following the decay of $^{123}Cd^{g}$ ($T_{1/2}=2.12$ s). The last column indicates the relative position in the level scheme shown in Fig. 3. The intensities are in percent of decays from the parent nucleus.

Energy (keV)	Error (keV)	Intensity	Error	Coincidences γ rays (keV)	Levels (keV) initial–final
243.96	0.30	0.37	0.22		
256.69	0.05	2.83	0.37		2393–2137
347.48	0.08	2.97	0.47	371,1331	2377–2030
353.63	0.07	3.62	0.40	371,1084,1341	1052–699
363.67	0.60	0.25	0.02		2393–2030
371.32	0.03	52.40	3.13	439,603,615,917 1228,1331,1438,1460 1695,1731,1831,1843	699–327
438.68	0.05	2.32	0.25	371,999,1256	1138–699
454.25	0.05	0.25	0.03	1566	2021–1566
512.00	0.50	0.41	0.08		2541–2030
525.20	0.20	1.01	0.14		
545.40	0.30	2.64	0.22		
602.73	0.03	1.22	0.02	1228	2529–1926
615.10	0.90	1.39	0.13		2541–1926
714.00	0.25	0.46	0.14		
810.29	0.03	6.27	0.59	883,999,1256	1138–327
813.63	0.09	1.88	0.26		2430–1616
827.23	0.25	0.33	0.15		2393–1566
881.17	0.05	4.36	0.87	1512	2393–1512
883.00	0.90	0.25	0.06	810	2021–1138
913.41	0.15	2.04	0.35		
917.16	0.06	4.41	0.48		1616–699
999.12	0.15	1.42	0.26		2137–1138
1044.88	0.12	1.74	0.27		
1052.28	0.03	25.07	1.59	1084,1341,1489	1052–0
1084.32	0.03	4.96	0.38	1052	2137–1052
1227.50	0.05	2.48	0.24		1926–699
1255.65	0.05	2.62	0.21		2393–1138
1288.35	0.20	0.38	0.07		1616–327
1324.77	0.15	1.39	0.26		2377–1052
1331.44	0.05	6.62	0.59	371	2030–699
1341.06	0.05	3.05	0.27	1052	2393–1052
1377.36	0.10	1.39	0.20		2430–1052
1403.37	0.15	0.44	0.11		2541–1138
1438.13	0.05	8.42	0.67	371	2137–699
1460.07	0.05	4.10	0.31		2159–699
1488.91	0.05	2.62	0.26		2541–1052
1512.09	0.05	4.28	0.25	881	1512–0
1519.48	0.10	1.09	0.16		
1566.09	0.05	0.33	0.02	454	1566–0
1594.81	0.65	0.63	0.06		
1599.23	0.12	1.17	0.19		1926–327
1641.86	0.20	0.63	0.13		
1694.81	0.05	7.08	0.49	371	2393–699
1702.37	0.07	2.21	0.26		2030–327
1730.95	0.06	1.99	0.19		2430–699
1809.50	0.09	1.72	0.18		2137–327
1830.78	0.05	6.05	0.42	371	2529–699
1842.86	0.05	7.79	0.54	371	2541–699
1976.00	0.10	2.18	0.30		
2020.71	0.05	0.71	0.05	No coincidences	2021–0
2202.14	0.07	3.16	0.31		2529–327
2214.33	0.10	1.61	0.21	No coincidences	2541–327
2393.46	0.15	0.71	0.02		2393–0

TABLE II. γ-ray energies and intensities following the decay of $^{123}Cd^m$ ($T_{1/2}=1.81$ s). The last column indicates the relative position in the level scheme shown in Fig. 4. The intensities are in percent of decays from the parent nucleus. An intensity error 0.00 means that it is less than 0.01.

Energy (keV)	Error (keV)	Intensity	Error	Coincidences γ rays (keV)	Levels (keV) Initial–Final
84.70	0.35	0.20	0.10	935,1166	2186–2101
107.10	0.30	0.14	0.05		2462–2355
138.38	0.10	0.87	0.15	935,1028,1102,1364	1166–1027
174.79	0.06	2.24	0.31	2355	2529–2355
193.39	0.40	0.42	0.18		2724–2529
207.12	0.10	1.35	0.25	2103	2310–2103
226.36	0.09	0.60	0.07		
256.69	0.05	0.23	0.02		2393–2137
261.50	0.50	0.93	0.10	1028,1102,1166,1240	2529–2268
292.90	0.10	0.41	0.04		2602–2310
299.90	0.20	0.18	0.03		
334.03	0.05	0.78	0.06	2021	2355–2021
353.63	0.07	0.05	0.00	371,1084,1341	1052–699
371.32	0.03	0.89	0.05	439,1438,1695	699–327
428.41	0.03	7.33	0.43	935,1166	2529–2101
438.68	0.05	0.24	0.03	371,999,1256	1138–699
454.25	0.05	0.69	0.07		2021–1566
459.55	0.06	0.47	0.06		
480.28	0.03	1.34	0.10	454,2021	2501–2021
514.95	0.50	0.62	0.04		2618–2103
646.00	0.30	0.20	0.04		
672.09	0.15	0.19	0.05		
684.25	0.20	0.17	0.05		
810.29	0.03	0.71	0.05	883,999,1256	1138–327
827.23	0.30	0.02	0.01		2393–1566
881.17	0.05	0.36	0.07	1512	2393–1512
883.00	0.10	0.54	0.01	810	2021–1138
935.10	0.03	10.41	0.62	428,1166	2101–1166
987.60	0.10	1.23	0.27	1474	2462–1474
988.73	0.10	4.66	0.26	1512	2501–1512
999.12	0.15	0.02	0.00		2137–1138
1012.91	0.10	1.95	0.25		2179–1166
1027.50	0.03	22.23	1.46	138,1151,1240,1282, 1474,1502	1027–0
1052.28	0.03	0.30	0.01	1084,1341	1052–0
1084.32	0.03	0.07	0.00	1052	2137–1052
1102.20	0.03	3.03	0.21		2268–1166
1143.84	0.15	1.10	0.23		2310–1166
1150.81	0.60	0.41	0.21		2179–1027
1165.86	0.03	25.18	1.51	935,1013,1102,1144, 1189,1364,1452,1558	1166–0
1177.70	0.20	0.23	0.02		
1188.79	0.09	0.46	0.06		2355–1166
1240.48	0.03	7.90	0.47	1028	2268–1027
1255.65	0.05	0.22	0.01		2393–1138
1275.73	0.35	0.88	0.07		
1282.19	0.04	3.30	0.19		2310–1027
1307.18	0.05	0.73	0.07		
1341.06	0.05	0.27	0.02	1052	2393–1052
1363.64	0.03	4.59	0.27	1166	2529–1166
1438.13	0.05	0.11	0.00	371	2137–699
1452.00	0.05	1.09	0.10		2618–1166
1473.77	0.03	7.20	0.51	1028	2501–1027
1473.77	0.03	1.23	0.08	989	1474–0
1502.13	0.15	0.31	0.05		2529–1027
1512.09	0.03	4.56	0.27	881,989	1512–0
1557.74	0.05	1.14	0.09	1166	2724–1166

TABLE II. (*Continued*).

Energy (keV)	Error (keV)	Intensity	Error	Coincidences γ rays (keV)	Levels (keV) Initial–Final
1566.09	0.05	1.93	0.01	454	1566–0
1694.81	0.05	0.55	0.03	371	2393–699
1809.50	0.09	0.03	0.00		2137–327
2009.08	0.15	0.26	0.04		
2020.71	0.04	2.02	0.10	334,480	2021–0
2102.81	0.05	12.31	0.73		2103–0
2111.29	0.06	1.44	0.12		
2151.52	0.20	0.14	0.03		
2178.98	0.15	0.28	0.04		2179–0
2268.09	0.10	0.53	0.06		2268–0
2308.41	0.15	0.49	0.07		
2354.74	0.06	7.26	0.43	107,175	2355–0
2393.46	0.15	0.06	0.00		2393–0
2408.16	0.07	1.93	0.62		
2461.50	0.07	7.94	0.47	No coincidences	2462–0
2500.44	0.09	0.62	0.06		2501–0
2601.98	0.08	11.77	0.71	No coincidences	2602–0
3077.73	0.30	0.15	0.02		

TABLE III. γ-ray energies and intensities following the decay of ^{125}Cd^{g} ($T_{1/2}=0.68$ s). The last column indicates the relative position in the level scheme shown in Fig. 5. The intensities are in percent of decays from the parent nucleus.

Energy (keV)	Error (keV)	Intensity	Error	Coincidences γ rays (keV)	Levels (keV) Initial–Final
267.88	0.25	1.46	0.50		
294.38	0.15	1.44	0.28		
302.96	0.15	1.90	0.16		1099–797
361.10	0.25	0.69	0.19		
369.23	0.15	0.85	0.18		1589–1220
389.45	0.15	2.34	0.48		
422.91	0.10	3.15	0.40		1220–797
436.29	0.03	42.50	2.55	303,423,792,1014, 1350,1553,1585,1701, 1788,1844	797–360
445.32	0.20	1.40	0.38		
538.87	0.40	0.33	0.08		2349–1811
551.46	0.25	0.51	0.21		
687.28	0.15	2.96	0.41		2498–1811
774.46	0.20	1.18	0.29		2585–1811
792.43	0.20	3.27	1.34		1589–797
799.00	0.35	1.79	0.43		
859.71	0.05	6.79	0.06	1365	1220–360
996.78	0.10	4.77	0.64		2585–1589
1013.97	0.10	3.91	0.98		1811–797
1099.48	0.03	25.63	2.13		1099–0
1249.75	0.25	2.22	0.36		2349–1099
1256.65	0.45	0.48	0.22		
1275.15	0.05	0.87	0.39		
1349.93	0.50	1.77	0.50		2147–797
1364.64	0.20	2.76	0.20		2585–1220
1421.67	0.15	1.46	0.34		2641–1220
1552.88	0.15	2.91	0.36		2349–797
1584.83	0.05	8.34	0.71	436	2381–797
1700.96	0.05	12.36	0.92	436	2498–797
1788.38	0.20	0.95	0.25		2585–797
1844.43	0.20	2.02	0.40		2641–797
1989.50	0.15	1.87	0.32		2349–360

FIG. 3. (*Continued*).

Energy (keV)	Error (keV)	Intensity	Error	Coincidences γ rays (keV)	Levels (keV) initial–final
2021.16	0.15	1.29	0.29		2381–360
2115.58	0.15	2.49	0.72		
2133.25	0.15	3.87	0.55		
2147.19	0.10	21.91	1.31		2147–0
2290.26	0.15	3.30	0.39		
2380.24	0.25	1.59	0.29		
2938.70	0.40	0.76	0.21		

TABLE IV. γ-ray energies and intensities following the decay of $^{125}Cd^{m}$ ($T_{1/2}=0.48$ s). The last column indicates the relative position in the level scheme shown in Fig. 6. The intensities are in percent of decays from the parent nucleus.

Energy (keV)	Error (keV)	Intensity	Error	Coincidences γ rays (keV)	Levels (keV) Initial–Final
132.83	0.10	0.29	0.08		
146.38	0.20	2.42	0.36	737,1028	1173–1028
153.78	0.20	0.25	0.11	2065	2218–2065
160.03	0.15	0.36	0.07		2378–2218
164.28	0.25	0.18	0.06		
191.88	0.15	2.13	0.34	737,1173	2102–1910
238.97	0.15	0.64	0.14		2616–2378
247.53	0.03	2.89	0.26	1219,1365,2392	2640–2392
262.15	0.03	2.04	0.22	1351,1028	2640–2378
276.85	0.30	0.25	0.07		
281.55	0.15	0.81	0.11		2253–1971
286.83	0.20	0.43	0.12		
313.47	0.20	0.69	0.14		2378–2065
341.34	0.08	0.80	0.09		
345.86	0.08	0.60	0.08		
391.30	0.15	0.32	0.07		
407.46	0.08	0.70	0.09		2378–1971
445.32	0.20	0.38	0.10		
453.70	0.15	0.35	0.07		
482.80	0.08	0.78	0.09		
524.28	0.15	0.37	0.07		
529.66	0.20	0.74	0.10		
536.48	0.08	0.91	0.10		1564–1028
543.10	0.08	0.78	0.09		
549.29	0.30	0.37	0.16		2802–2253
555.10	0.10	0.23	0.12		
570.52	0.15	0.52	0.09		
577.36	0.15	0.55	0.09		2642–2065
606.52	0.10	0.74	0.11		
626.81	0.25	0.33	0.08		
646.11	0.15	0.89	0.12		
683.64	0.04	2.07	0.17		2642–1958
707.01	0.35	0.26	0.08		
716.00	0.15	0.94	0.18		
721.88	0.08	1.36	0.14		2632–1910
730.73	0.08	1.78	0.19		2640–1910
736.65	0.03	13.85	0.83	192,722,731,909, 1173	1910–1173
753.76	0.25	0.27	0.11		
909.10	0.08	1.50	0.17	737,1173	2819–1910
928.40	0.10	1.18	0.18		2102–1173
1027.53	0.08	28.43	1.71	146,536,1221,1351, 1365,1589,1614	1028–0
1044.72	0.04	3.85	0.34	1173	2218–1173

TABLE IV. (*Continued*).

Energy (keV)	Error (keV)	Intensity	Error	Coincidences γ rays (keV)	Levels (keV) Initial–Final
1064.26	0.08	2.19	0.24		2642–1578
1075.44	0.25	0.97	0.17		2249–1173
1106.50	0.50	0.37	0.30		
1113.19	0.50	0.70	0.45		
1173.16	0.03	27.58	1.65	737,909,928,1045, 1075,1219,1238,1467	1173–0
1205.19	0.10	1.05	0.16		2378–1173
1219.08	0.15	1.78	0.36	1173	2392–1173
1221.09	0.25	1.19	0.53		2249–1028
1238.41	0.08	1.58	0.18		2412–1173
1351.08	0.10	1.80	0.20	262,1028	2378–1028
1364.64	0.20	1.10	0.20		2392–1028
1399.69	0.05	2.20	0.21		2574–1173
1467.35	0.03	3.32	0.23		2640–1173
1563.86	0.08	1.08	0.11		1564–0
1577.66	0.05	2.65	0.21	1064	1578–0
1589.11	0.05	2.91	0.24	1028	2616–1028
1613.74	0.08	12.09	1.25	1028	2642–1028
1719.34	0.30	0.25	0.06		
1774.90	0.20	0.55	0.10		2802–1028
1835.88	0.25	0.35	0.06		2863–1028
1898.28	0.40	0.38	0.20		
1909.94	0.15	0.74	0.11		1910–0
1958.29	0.08	2.33	0.18		1958–0
1971.09	0.10	1.70	0.16	407	1971–0
2064.64	0.05	3.92	0.29	154,313,577	2065–0
2101.06	0.15	0.48	0.12		2102–0
2252.80	0.15	1.20	0.12		2253–0
2360.80	0.25	0.38	0.08		
2392.43	0.03	10.30	0.80	248	2392–0
2616.26	0.03	5.25	0.37		2616–0

masses these cycles were repeated during several hours of continuous irradiation.

Energy calibrations were made using the standard lines of the ^{241}Am, ^{57}Co, ^{133}Ba, ^{137}Cs, ^{60}Co, and ^{24}Na sources. Single- and double-escape γ-ray lines from the last source were also employed. Calculations and fittings were made using the code CALIB.[19]

Efficiency calibrations over the range 0.2–3.0 MeV were performed by collecting mass 138 activity on-line with the same geometry as used during measurements.[20] The low-energy part of the efficiency calibration curve was completed by means of measurements with ^{241}Am and ^{57}Co standard sources.

Single γ-ray and multiscaling spectra, together with the bidimensional coincidences spectra were recorded on-line in order to be analyzed off-line.

III. EXPERIMENTAL RESULTS

The identification of the γ radiation associated with the ^{123,125}Cd decays was performed using the activity ratios obtained from two sets of single γ-ray spectra (one set for each isotope decay) recorded with different collector assemblies as mentioned in the preceding section. Figures 1(a) and (b) show the most relevant part of the two single-γ-ray on-line spectra recorded with the collecting tape moving continuously, enhancing the ^{123,125}Cd decay activities with respect to the ^{123,125}In and ^{123,125}Sn decay activities.

A. Mass 123

Two half-lives were observed and measured in the decays of ^{123}Cd. The corresponding value from the low-spin isomer decay was 2.12±0.03 s in good agreement with Refs. 13 and 15 while the value corresponding from the high-spin isomer decay, was 1.81±0.03 s in close agreement with Ref. 15. The γ rays used for these measurements were the 371 and 1052 keV transitions, and the 935, 1028, and the 1166 keV transitions for the 2.12 and 1.81 s half-lives, respectively. Decay curves for the most important γ transitions are shown in Fig. 2(a).

Based upon systematic considerations obtained from Ref. 21, a $\frac{3}{2}^+$ spin and parity assignment is suggested for the ^{123}Cd low-spin isomer. As it would probably be the ground state, it will be tentatively referred to as ^{123}Cd^g. For the high-spin isomer a $\frac{11}{2}^-$ spin and parity assignment is also suggested based upon systematic, and it will be referred to as ^{123}Cd^m. No measurements were performed in order to obtain the relative energy position of both isomers.

The results for the different decays from the two ^{123}Cd isomers are summarized in Tables I and II with the observed γ-ray energies and intensities along with their errors, the coincidence relations and the relative positions in the corresponding energy level schemes to be discussed in Sec. IV.

B. Mass 125

As in the foregoing case, two half-lives have been observed and measured. These are assigned to the decays from the low-spin isomer with value 0.68±0.04 s and from the high-spin isomer with value 0.48±0.03 s. This value is substantially different as compared to the previous reported half-life of 0.66±0.03 s.[15] The γ rays used were 436, 1099, and 1701 keV transitions and 1028 and

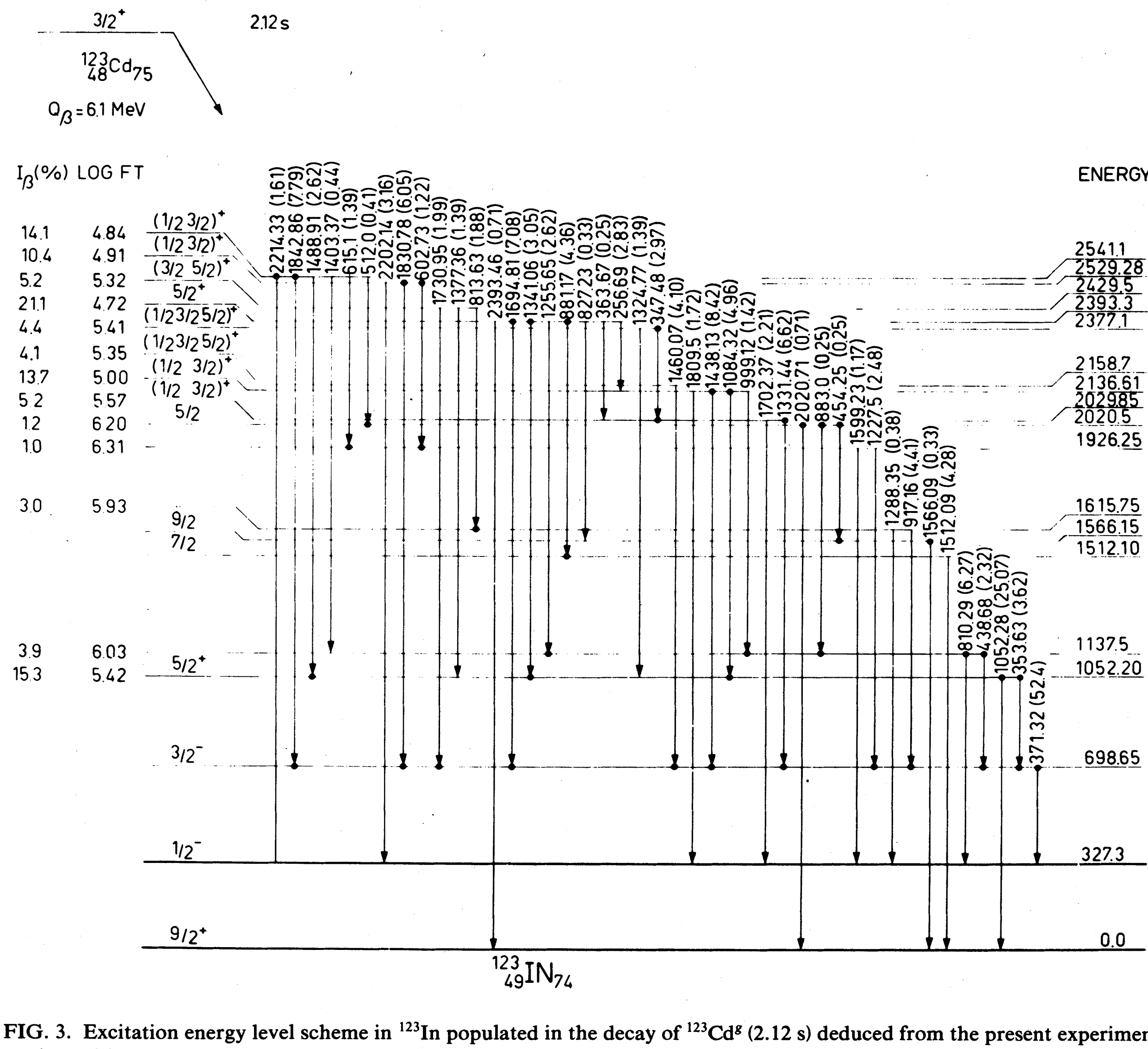

FIG. 3. Excitation energy level scheme in ^{123}In populated in the decay of ^{123}Cd^g (2.12 s) deduced from the present experiment. The γ-ray intensities are given in percent of the decays of the parent nucleus. A solid circle at an arrowhead indicates an observed coincidence relation, while a solid circle at the tail of an arrow means that the transition has been used as a coincidence gate. The Q_β values here and in Figs. 4–6 were taken from Ref. 23. Energy levels and γ-ray transition are in keV. The spins and parities of the ground and metastable states here and in Figs. 4–6 are suggested based upon systematic considerations obtained from Ref. 21.

1173 keV transitions for the 0.68 and 0.48 s half-lives, respectively. Decay curves of the most important γ transitions are shown in Fig. 2(b).

As in the previous case, systematic would suggest a $\frac{3}{2}^+$ for the probably ground-state low-spin isomer and a $\frac{11}{2}^-$ for the high-spin isomer. They will be referred to as ^{125}Cd^g and ^{125}Cd^m, respectively. The relative energy between both isomers is not known. In Tables III and IV a summary of the results obtained from the two different decay modes in ^{125}Cd are presented.

IV. THE LEVEL SCHEMES

Using the experimental results obtained in this work the decay schemes of ^{123}Cd^{g,m} and ^{125}Cd^{g,m} shown in Figs. 3–6 are proposed. The corresponding energy level schemes of ^{123}In and ^{125}In were based upon γ-γ coincidence relations, energy sums, and intensity balances. When γ rays showed no coincidences they were placed in the scheme as transitions to previously established levels.

The β-feeding percent intensity for each level was calculated from the relative intensities deduced from the single γ-ray spectra supposing no β feeding to the ground and isomeric states. Logft values have been calculated using the formulas and tables of Ref. 22 and the Q_β values were obtained from Ref. 23.

The spins and parities suggested for each level were based upon logft values, systematic considerations, and the probable spins and parities of the levels connected through the γ transitions with the level involved. Some levels have up to three possible spins and no spin suggestions were made for more than this level of uncertainty.

Our level schemes are not substantially different from those of Ref. 13 as far as the position of the different levels and the most important γ-ray transitions are concerned. Nevertheless, since in this work a $\frac{11}{2}^-$ isomeric state is suggested by systematic considerations for both ^{123}Cd and ^{125}Cd, the present spin and parity assignments of some relevant levels are rather different from those of Ref. 13. Furthermore, the present assignments are in good agreement with our theoretical calculations based

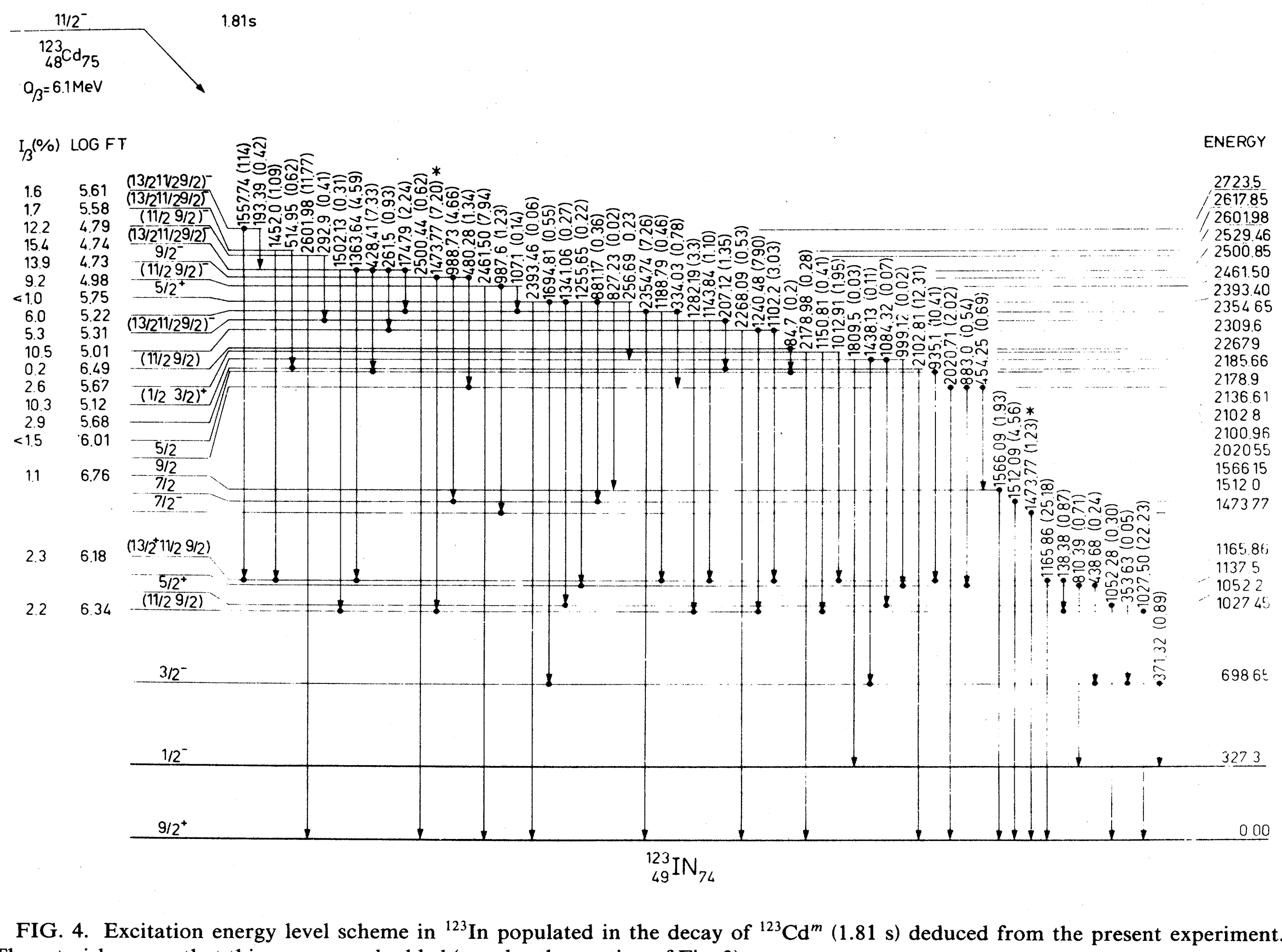

FIG. 4. Excitation energy level scheme in ^{123}In populated in the decay of ^{123}Cd^m (1.81 s) deduced from the present experiment. The asterisk means that this γ ray was doubled (see also the caption of Fig. 3).

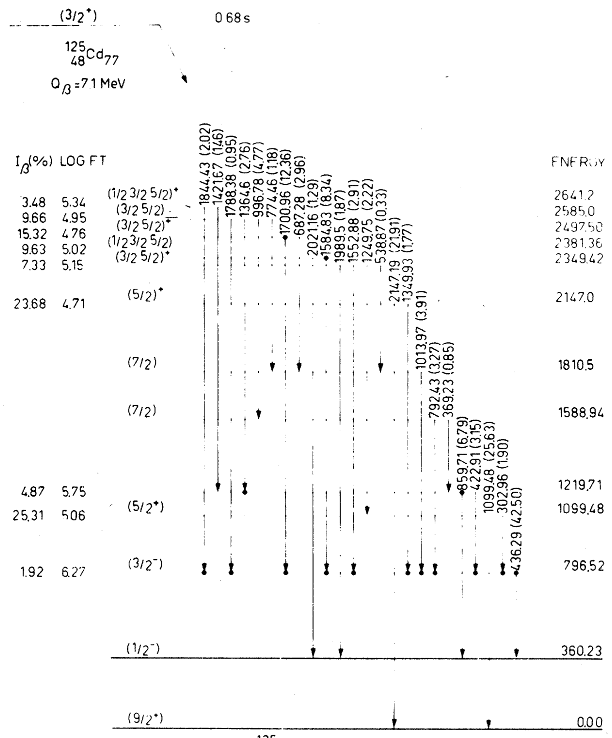

FIG. 5. Excitation energy level scheme in ^{125}In populated in the decay of ^{125}Cd^{g} (0.68 s) deduced from the present experiment (see also the caption of Fig. 3).

on the hole-vibration coupling as will be suggested in Sec. V.

A. Decay schemes of ^{123}Cd^{g} and ^{123}Cd^{m}

The decay scheme of ^{123}Cd^{g} with 2.12 s half-life consists of 43 γ-ray transitions including 94% of the relevant total γ-ray intensity. Those γ rays are arranged in 17 excited states of ^{123}In. The proposed level scheme was constructed starting from the 1052.2 keV level, determined by the 1052 keV γ-ray transition to the ground state, and the 354 keV transition to the second excited state, and from this level, through the 371 keV γ-ray transition, to the isomeric first excited state. In this fashion the energies of the first two excited states were determined at 327.3 and 698.7 keV, in reasonable agreement with the values determined in Ref. 2 using the ^{124}Sn(d,^{3}He)^{123}In pick-up reaction.

The spins and parities of the ground state, and the first and second excited states were also known from Ref. 2. The possible spins of the 1052 keV level deduced from logft values are $(\frac{1}{2},\frac{3}{2},\frac{5}{2})^{+}$. The suggested $\frac{5}{2}^{+}$ is enforced by its strong γ-ray transition to the $\frac{9}{2}^{+}$ ground state. Similar considerations were performed for the spin assignments of the 2021 and 2393 keV levels. The 1512 keV level is not β fed in any of the two decays, therefore its spin is very likely to be $\frac{7}{2}$.

In the decay scheme of ^{123}Cd^{m} with 1.81 s half-life 58 γ-ray transitions were identified for 25 excited states of ^{123}In exhausting more than 95% of the relevant γ-ray intensity. The proposed scheme was based upon the most intense γ-ray transitions belonging to this decay mode, the 1166 and 1028 keV transitions both decaying to the ground state. All the other excited states were placed by coincidence relations, energy sums, and intensity balances.

Suggested spins and parities for the 1027, 1166, and 2462 keV levels were made disregarding $\frac{13}{2}^{-}$ due to the obvious strong transition to the $\frac{9}{2}^{+}$ ground state. The level at 1474 keV is not fed from the $\frac{11}{2}^{-}$ isomeric state, so it is γ fed by the suggested $(\frac{9}{2},\frac{11}{2})^{-}$ level at 2462 keV and it deexcites to the $\frac{9}{2}^{+}$ ground state. Therefore, the suggested $\frac{7}{2}^{-}$ seems to be quite reasonable.

Considering the γ transition from the $\frac{5}{2}$ spin state at 2021 keV, a $\frac{11}{2}$ spin is not a good candidate for the 1566 keV level. The 2501 keV level seems to be a $\frac{9}{2}^{-}$ since it has a very strong β feeding from the $\frac{11}{2}^{-}$ state and also two γ transitions connecting the $\frac{5}{2}$ and the $\frac{7}{2}$ levels.

Only two states shared by the two decay schemes have been observed. These are the states at 2021 and 2393 keV. Both are β fed from the $\frac{3}{2}^{+}$ ground state of ^{123}Cd^{g} and therefore it is very improbable that they are also β fed from the $\frac{11}{2}^{-}$ of the ^{123}Cd^{m}. In this level scheme this is incompatible with the positive values of the $I_\beta(\%)$ obtained for both levels. The only possible explanation could be undetected low-energy γ-ray transitions feeding those levels from high-lying states in the scheme.

B. Decay schemes of ^{125}Cd^{g} and ^{125}Cd^{m}

The decay scheme of ^{125}Cd^{g} has 24 γ-ray transitions comprising 87% of the total γ-ray intensities observed in this decay. They connect 12 excited states in ^{125}In. Analog considerations such as those taken into account for the level scheme of ^{123}Cd^{g}, were invoked in order to construct the level scheme of the ^{125}Cd^{g} decay. The 1099 keV transition to the ground state defines the level at 1099.5 keV; from this level to 303 keV γ-ray transition to the second excited state determines this state at 796.5 keV. The strong γ-ray transition of 436 keV deexcites this level to the isomeric first excited state and determines the energy of this level at 360.2 keV. In this case there were no data available from nuclear reactions to compare, however, the values given for the first two energy levels in ^{125}In are in good agreement with that of Ref. 13.

The spins and parities suggested for the ground state and the two first excited states are based on systematic considerations only. A $\frac{7}{2}$ spin is very likely for the 1811 and 1589 keV levels because they are not β fed from the ground state of ^{125}Cd^{g}. The systematic would indicate that the spin and parity for the 1099 keV level is likely to be $\frac{5}{2}^{+}$. It also decays to the $\frac{9}{2}^{+}$ ground state and it has a very strong β feeding. The same arguments may be applied to the 2147 keV state.

The level scheme of the ^{125}Cd^{m} decay contains 49 γ-ray transitions connecting 23 excited states in ^{125}In exhausting 93% of the total γ intensity measured for this decay mode. It was built up by analogy with the decay scheme for ^{123}Cd^{m}. The most intense γ transitions, 1028 and 1173 keV, deexciting to the ground state, determine the energy of the corresponding excited levels in ^{125}In. This scheme has no shared levels with the ^{125}Cd^{g} decay scheme, making the intensity balances more easily performed.

The suggested spins are our most reliable values used in order to be consistent with logft values and with the γ-transitions connecting different levels. These arguments make a $\frac{13}{2}^{-}$ spin assignment very unlikely for the considered states.

V. DISCUSSION

The lower-energy states of many-body systems may be described in terms of a vacuum state and elementary (independent) excitations. In superfluid nuclei as the Sn isotopes the Bardeen-Cooper-Schrieffer (BCS) ground state constructed with a determinant wave function is the most common ground state. The first excited 2^{+} state of Sn has a collective character and is produced by a quadrupole surface vibration (phonon). From this point of view, the energy spectra of the ^{123}In and ^{125}In can be discussed as a proton hole coupled to the vibrating core of the near ^{124,126}Sn isotopes.

The Hamiltonian is assumed to be given by

$$H = H_0 + H_p + H_q \ ,$$

where

$$H_0 = \sum_{j,m} \varepsilon_j a^{\dagger}_{j,m} a_{j,m} \ ,$$

$$H_p = -G \sum_{j_1 > j_2} \sum_{\substack{m_1 > 0 \\ m_2 > 0}} a^{\dagger}_{j_1 m_1} a^{\dagger}_{j_1 - m_1} a_{j_2 - m_2} a_{j_2 m_2} \ ,$$

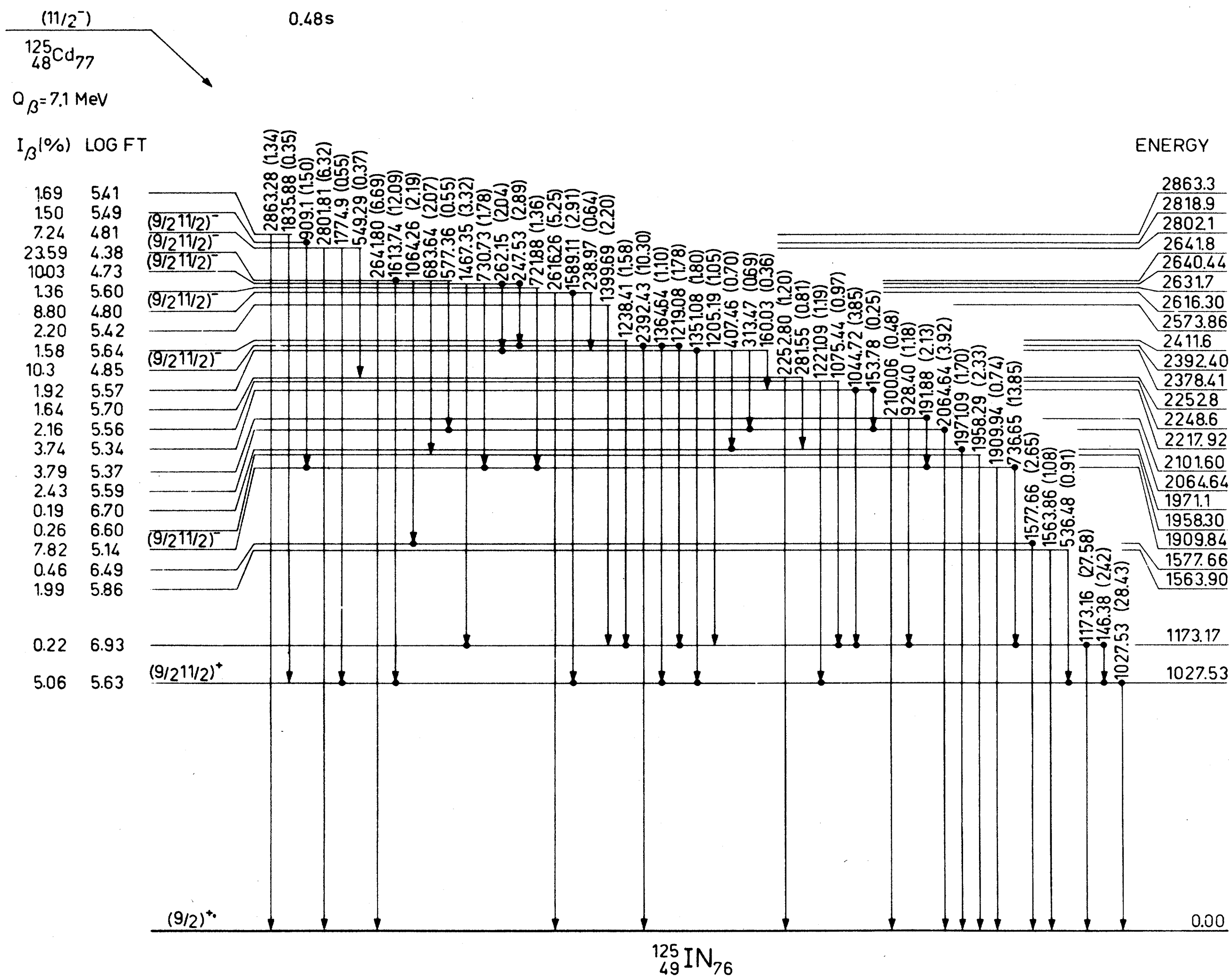

FIG. 6. Excitation energy level scheme in ^{125}In populated in the decay of ^{125}Cd^{m} (0.48 s) deduced from the present experiment (see also the caption of Fig. 3).

$$H_q=(-\kappa/2)\sum_{\mu} Q^{\dagger}_{\lambda\mu}Q_{\lambda\mu} ,$$

and $a^{\dagger}_{jm}$ creates a particle in an orbital j,m and

$$Q_\mu=[-1/(5)^{1/2}]\sum_{j_1 j_2}\langle j_1\|r^2Y_2\|j_2\rangle[a^{\dagger}_{j_1}a_{j_2}]_{2,\mu} .$$

The Hamiltonian H_0+H_p is diagonalized with a BCS transformation to quasiparticles

$$C^{\dagger}_{jm}=U_j a^{\dagger}_{jm}-V_j(-)^{j-m}a^{\dagger}_{jm} ,$$

obtaining a quasiparticle Hamiltonian

$$H=\sum_{jm}E_jC^{\dagger}_{jm}C_{jm}-(\kappa/2)\sum_{\mu}Q^{\dagger}_{\mu}Q_\mu .$$

This interaction was diagonalized in a basis of particle hole coupled to angular momentum 2 in a random phase approximation (RPA). The coupling constant κ was fixed by fitting the experimental energy of the first 2^+ excited states in ^{124,126}Sn. The next step is to calculate the energy spectra of the ^{123,125}In coupling the single proton-hole to one and two phonon states.

The interaction between the quasiparticle and the surface vibrations depends linearly on the collective deformation and the quasiparticle degrees of freedom. In terms of the magnitudes defined above one obtains

$$H_{\rm int}=-\kappa\sum_{\mu}(Q^{\dagger}_{\mu})_{\rm coll}Q_\mu ,$$

with $(Q^{\dagger}_{\mu})_{\rm coll}$ defined in terms of the first collective root of the RPA:

$$(Q^{\dagger}_{\mu})_{\rm coll}=\{[-(2\lambda+1)^{1/2}]/\kappa\}\Lambda(\Gamma^{\dagger}_{\mu}+\Gamma_{2\mu}(-)^{\mu}) ,$$

where $\Gamma^{\dagger}_{2\mu}$ creates a phonon of angular momentum and parity 2^+ and Λ is a normalization parameter fixed in the RPA.

Within the framework of the nuclear field theory,[24] $H_{\rm int}$ has been worked out to first order with one hole, one-hole–one-phonon, and one-hole–two-phonons states. The single-particle energies for the neutron states have been taken from Ref. 25. For the proton-hole states, the following independent particle energies used referred to the $(1g_{9/2})^{-1}$ ground state: 327 keV for the $(2p_{1/2})^{-1}$ first excited state and 699 keV for the $(2p_{3/2})^{-1}$ second excited state. All these assumptions are well supported by pick-up reactions on ^{124}Sn[2] and the systematic of the odd-mass In isotopes shown in Fig. 7. The results of our theoretical calculations are presented in Figs. 8 and 9, together with the experimental level schemes deduced in the present work.

In ^{123}In the group of levels at approximately 1 MeV may be very well accounted for as interactions of in-

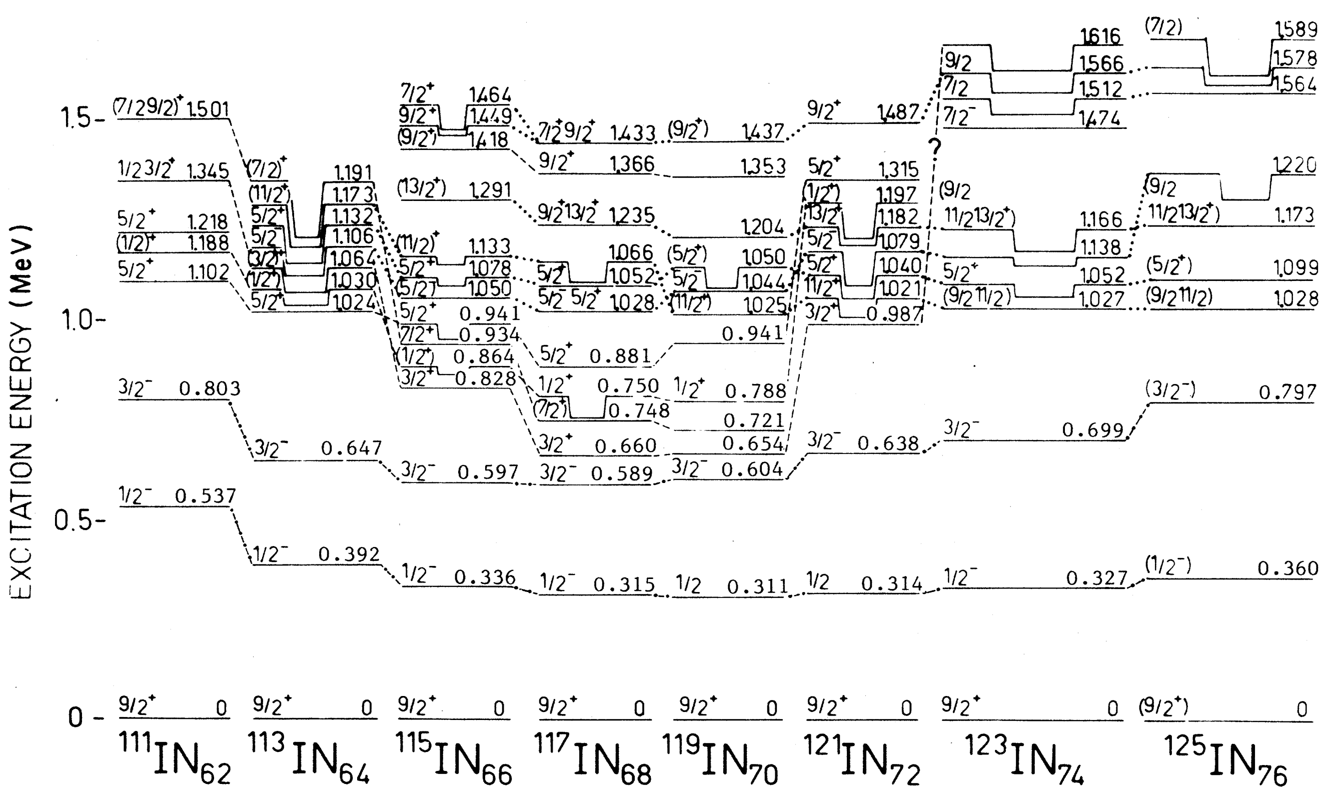

FIG. 7. Systematic of the low-lying excitation levels in odd-mass In nuclei from $A=111$ to 125. —·—·—·, single proton-hole states; · · · ·, members of the quintuplet $|(1g_{9/2})^{-1}\otimes 2^+;J\rangle^+$ and the $\frac{5}{2}^-$ member of the doublet $|(p_{1/2})^{-1}\otimes 2^+;J\rangle^-$ states; — — — rotational deformed states.

dependent particle states with the 2^+ quadrupole vibration of the ^{124}Sn core. Therefore, the possible structure of the 1027, 1052, and 1166 keV levels are consistent with the $\frac{11}{2}^+$, $\frac{5}{2}^+$, and $\frac{13}{2}^+$ or $\frac{9}{2}^+$ (respectively) members of the quintuplet $|(1g_{9/2})^{-1}\otimes 2^+;J\rangle^+$ (see Fig. 8). Further assignments, not shown in Fig. 8, might be suggested following our theoretical calculations. The 1138 keV level might be a $\frac{5}{2}^-$ which is also consistent with the systematic shown in Fig. 7. It is very likely a member of the doublet resultant from the $(2p_{1/2})^{-1}$,2^+ coupling. The configuration of the 1474 keV level is predominantly $|(2p_{3/2})^{-1}\otimes 2^+;J\rangle^-$ in good agreement with the $\frac{7}{2}^-$ assignment. The 1512 and 1566 keV levels may be the resting members of the $|(1g_{9/2})^{-1}\otimes 2^+;J\rangle^+$ quintuplet. The lowest energy $\frac{3}{2}^+$ state candidate, positioned at 1616 keV might be a member of an intruder band, but it has also a great chance to be the member of the $|(2p_{3/2})^{-1}\otimes 2^+;J\rangle^-$ quadruplet (see Fig. 8).

The structure of some levels around and above 2 MeV may be explained as the result of one-hole–two-phonons interactions. As an example, the 2393 keV level is very likely one of the $\frac{5}{2}^+$ members of the configuration $|(1g_{9/2})^{-1}\otimes(2^+\otimes 2^+)_j;J\rangle^+$. This is reinforced by the strong γ transition to the one-hole–one-phonon state positioned at 1052 keV (see Figs. 8 and 3). For the high-spin negative-parity states around 2.5 MeV a strong $|(1g_{9/2})^{-1}\otimes 3^-;J\rangle^-$ character is suggested since the even-mass neighborhood Sn isotopes have a 3^- state at

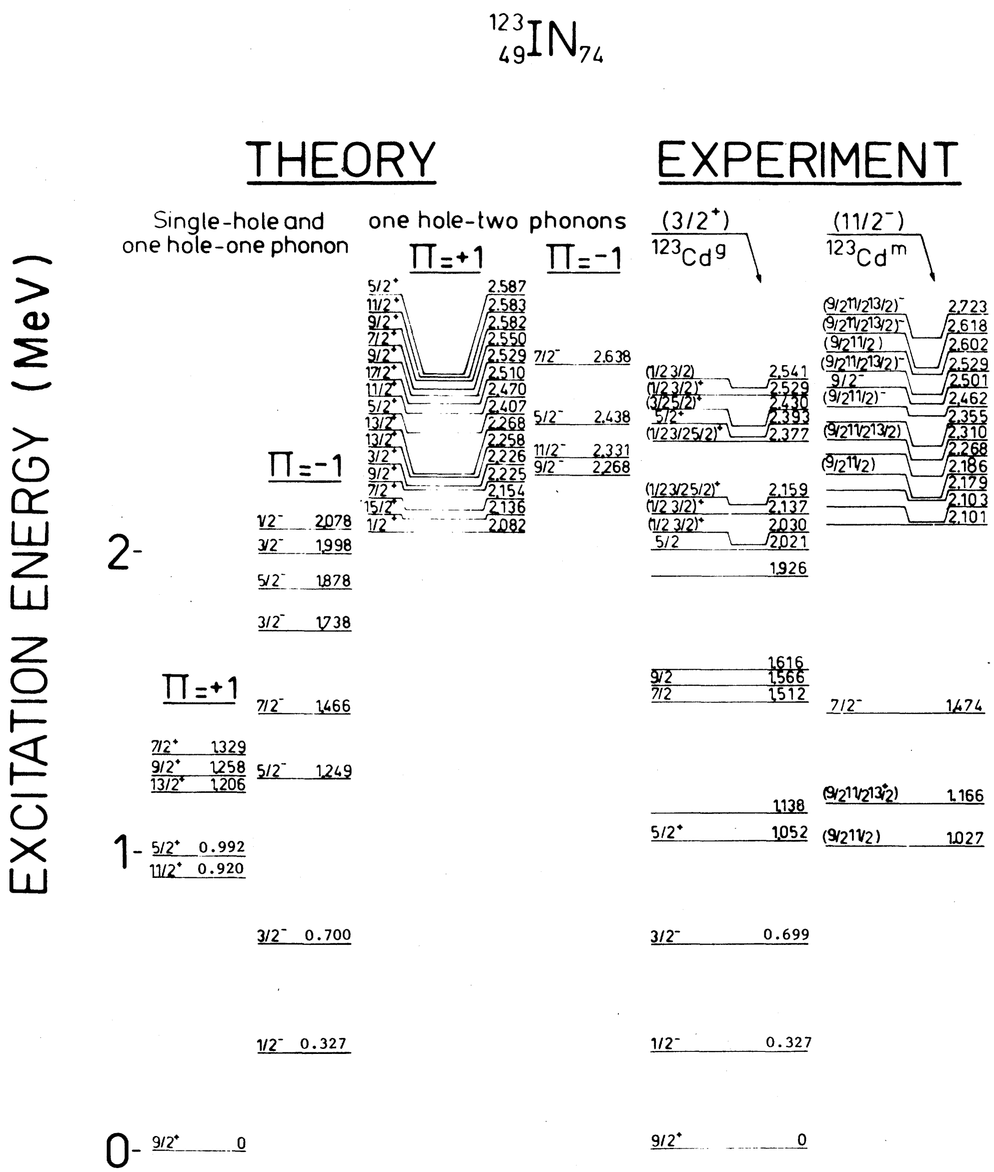

FIG. 8. The positive- and negative-parity excited levels of $^{123}_{49}$In$_{74}$ calculated in the single hard-core coupling model are compared with the experimental deduced levels.

approximately 2.5 MeV.

The ^{125}In nuclear structure is very similar to that of ^{123}In. Systematic considerations may be also argued in this case in order to consider the ground state, the 360 and the 797 keV levels as the single-particle states $(1g_{9/2})^{-1}$, $(2p_{1/2})^{-1}$, and $(2p_{3/2})^{-1}$, respectively. The same arguments as for ^{123}In are invoked to say that the 1028, 1099, and 1173 keV levels are members of the quintuplet $|(1g_{9/2})^{-1}\otimes 2^+;J\rangle^+$. The (probably) resting members are the 1564 and 1578 keV levels (see Fig. 9). The levels positioned at 1220 keV ($\frac{5}{2}^-$) and at 1589 keV ($\frac{7}{2}^-$) would have $|(2p_{1/2})^{-1}\otimes 2^+;J\rangle^-$ and $|(2p_{3/2})^{-1}\otimes 2^+;J\rangle^-$ configurations, respectively (see Fig. 9).

The arguments given before are in good agreement with the odd-mass In systematic already mentioned and shown in Fig. 7, where the same structure levels belonging to the different isotopes are joined by dotted or dashed lines. The rotational deformed states are also indicated (see caption of Fig. 7). In this way, any possible low-lying $\frac{3}{2}^+$ deformed state would be above 2 MeV of excitation energy in agreement with the systematic behavior of that level in the In isotopes.

VI. CONCLUSIONS

In this work it is demonstrated that the systematic behavior of the odd-mass Cd isotopes beyond $A = 121$ con-

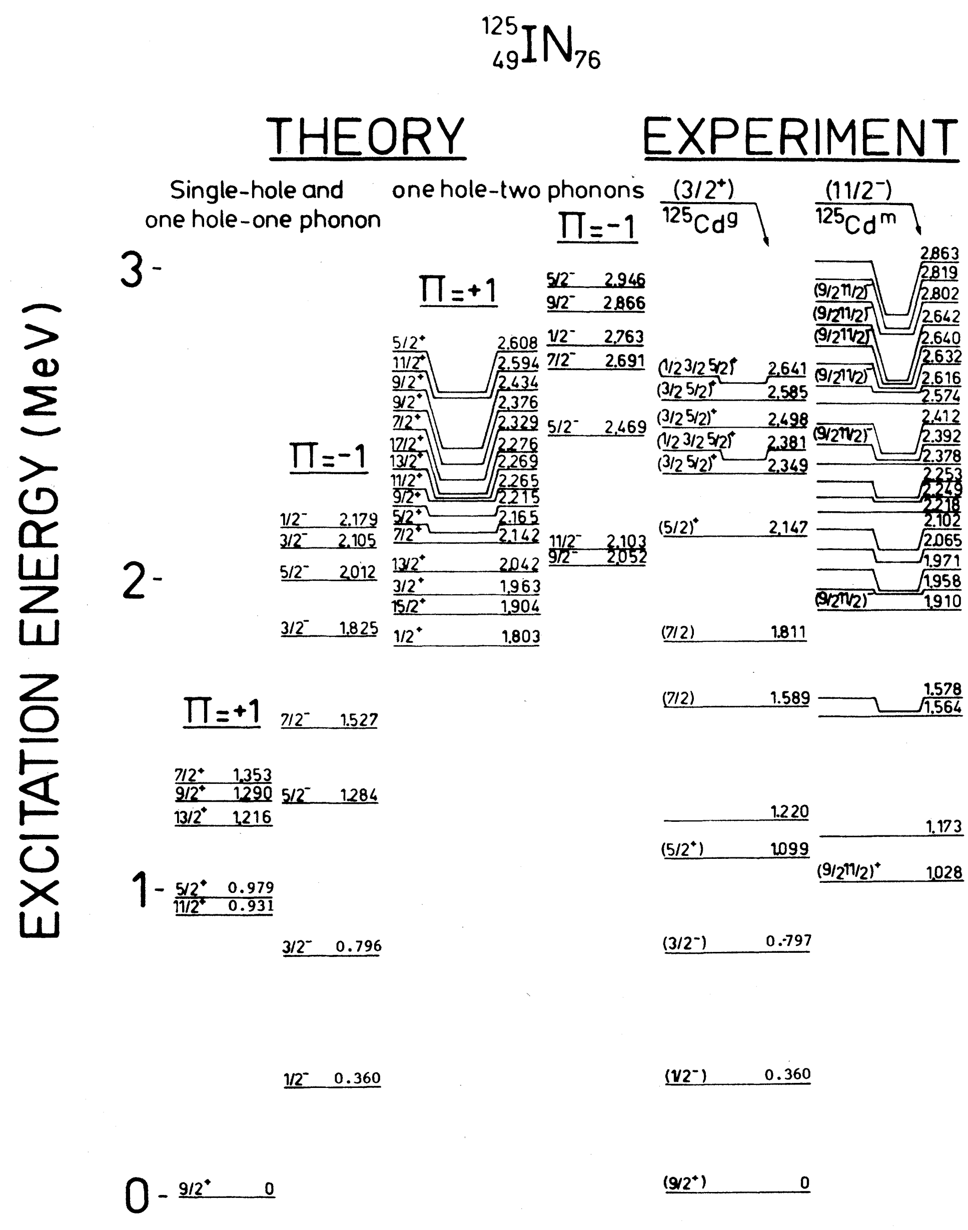

FIG. 9. The same as for Fig. 8 but for $^{125}_{49}$In$_{76}$ (see caption of Fig. 8).

tinues to show two β^- decaying isomers. The half-lives of the different decay modes from ^{123}Cd and ^{125}Cd have been measured giving values of 1.81 and 0.48 s for the isomeric states in ^{123}Cd and ^{125}Cd, respectively. Level schemes have been proposed for ^{123,125}In.

It has also been shown that the low-lying levels structure in ^{123}In and ^{125}In may be understood in terms of single-hole and quadrupole core vibrations coupled through a quadrupole particle-hole interaction, disregarding rotational deformed intruder states, at least for energies below 1.6 MeV in ^{123}In and 2 MeV in ^{125}In. This is in agreement with the assumption of decreasing deformation character for these nuclei when the numbers of neutrons approaches $N=82$. As is well known the deformation is due to quadrupole proton-neutron interaction and it depends on the number of pairs of protons and neutrons out of closed shell. In the case that the number of particles is over the middle of the shell, the interaction depends on the number of pairs of proton holes and neutron holes. This is the case when going from ^{121,123}In to ^{123,125}In, one pair of neutron holes decreases with the increasing number of neutrons. Therefore the deformation decreasing character is certainly associated with the increasing number of neutrons.

[1]M. Conjeaud, S. Harar, and E. Thuriere, Nucl. Phys. **A129**, 10 (1969).
[2]C. V. Weiffenbach and R. Tickle, Phys. Rev. C **3**, 1668 (1971).
[3]S. Harar and R. N. Horoshko, Nucl. Phys. **A183**, 161 (1972).
[4]J. W. Smits and R. H. Siemssen, Nucl. Phys. **A261**, 385 (1976).
[5]A. Bäcklin, B. Fogelberg, and S. G. Malmskog, Nucl. Phys. **A96**, 539 (1967).
[6]V. R. Pandharipande, K. E. Prasad, R. P. Sharma, and B. V. Thosar, Nucl. Phys. **A109**, 81 (1968).
[7]V. Sergeev *et al.*, Nucl. Phys. **A202**, 385 (1973).
[8]J. McDonald, B. Fogelberg, A. Bäcklin, and Y. Kawase, Nucl. Phys. **A224**, 13 (1974).
[9]C. W. Tang *et al.*, Z. Phys. A **272**, 301 (1975).
[10]M. D. Glascock *et al.*, Phys. Rev. C **20**, 2370 (1979).
[11]B. Fogelberg and P. Hoff, Nucl. Phys. **A376**, 389 (1982).
[12]Dietrich, A. Bäcklin, C. O. Lannergård, and I. Ragnarsson, Nucl. Phys. **A253**, 429 (1975).
[13]P. Hoff, B. Ekström, H Göktürk, and B. Fogelberg, Nucl. Phys. **A459**, 35 (1986).
[14]B. Fogelberg (private communication).
[15]H. Mach, R. L. Gill, D. D. Warner, A. Piotrowski, and R. Moreh, Phys. Rev. C **34**, 1117 (1986).
[16]M. Ballestero *et al.*, Nucl. Instrum. Methods Phys. Res. B **26**, 125 (1987).
[17]E. Perez Ferreira *et al.*, Nucl. Instrum. Methods **184**, 161 (1981).
[18]H. Huck *et al.*, Nucl. Instrum. Methods **189**, 347 (1981).
[19]E. Achterberg, Ph.D. thesis, Universidad de Cuyo, Argentina, 1979 (unpublished).
[20]E. Achterberg *et al.*, Nucl. Instrum. Methods **116**, 453 (1973).
[21]B. Fogelberg and P. Hoff, Nucl. Phys. **A391**, 445 (1982).
[22]N. B. Gove and M. J. Martin, Nucl. Data Tables **10**, No. 3, 206 (1971).
[23]L. Spanier, K. Aleklett, B. Ekström, and B. Fogelberg, Nucl. Phys. **A474**, 359 (1987).
[24]D. R. Bes, G. G. Dussel, R. A. Broglia, and R. Liotta, and B. R. Mottelson, Phys. Lett. **52B**, 253 (1974); D. R. Bes, R. A. Broglia, G. G. Dussel, R. J. Liotta, and H. M. Sofia, Nucl. Phys. **A260**, 27 (1976); D. R. Bes, R. A. Broglia, G. G. Dussel, R. J. Liotta, and R. P. J. Perazzo, Nucl. Phys. **A260**, 77 (1976).
[25]R. A. Uher and R. A. Sorensen, Nucl. Phys. **86**, 1 (1966).